

7 **S** Supporting Information



65 immunocompromised individuals, and may be better suited for
66 repeat use.

67 While peptide-based vaccines successfully administer the
68 minimal amount of pathogenic material necessary to elicit an
69 immune response, they often suffer from poor immunoge-
70 nicity. Success in vivo is contingent upon co-administration of
71 immune-stimulating adjuvants. It has been shown by us and
72 others that covalent conjugation of adjuvants to peptide
73 vaccines is an effective means of achieving enhanced immune
74 responses compared to admixtures of individual components,
75 as this minimizes the separation of adjuvant and antigen in
76 vivo, potentiating immunogenicity.^{19–26} When considering
77 vaccines for pulmonary delivery, immune recognition receptors
78 should be selected that may be accessed at the pulmonary
79 mucosa and safely stimulated. Previous work in our laboratory
80 demonstrated the successful use of powdered pulmonary
81 vaccines, consisting of proteins from Mtb noncovalently
82 associated with a TLR2-ligand, as a safe and effective
83 immunization strategy for TB.²⁷ TLR2 agonists may be
84 particularly suitable for use in the pulmonary environment, as
85 the receptor is expressed on multiple cell types, including both
86 antigen-presenting cell subsets and pulmonary epithelial
87 cells.^{28–30} Of particular interest, a recent study demonstrated
88 the protective potential of lipopeptide combinations from the
89 Mtb protein antigen ESAT6 (Rv3875).³¹ We reasoned
90 therefore that covalent conjugation of peptide epitopes from
91 Mtb to a TLR2-ligand would lead to an effective self-
92 adjuvanted vaccine that may be more stable while providing
93 a robust immunological response.

94 ■ RESULTS AND DISCUSSION

95 Toward this end, we designed a self-adjuvanted vaccine
96 candidate **1** (Figure 1) based on the covalent conjugation of

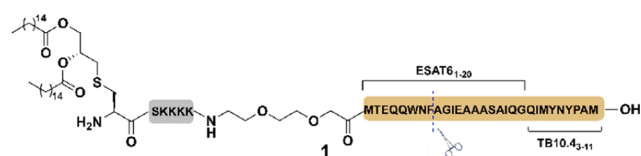
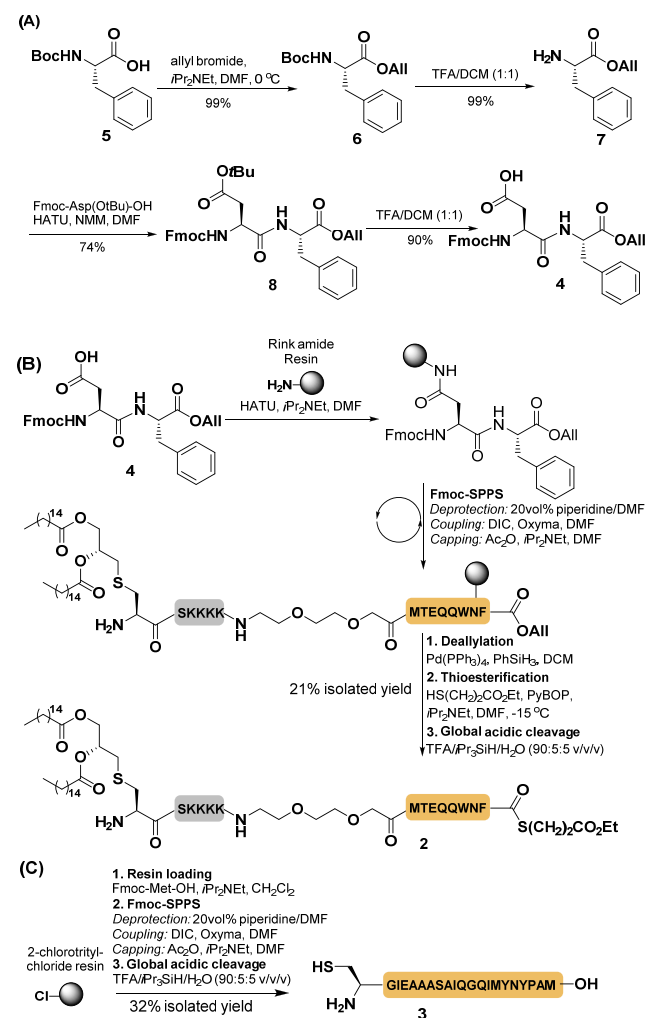


Figure 1. Self-adjuvanted vaccine candidate **1**, covalently conjugated Pam₂Cys as adjuvant and immunodominant T-lymphocyte epitopes from Mtb, ESAT6_{1–20} and TB10.4_{3–11}.

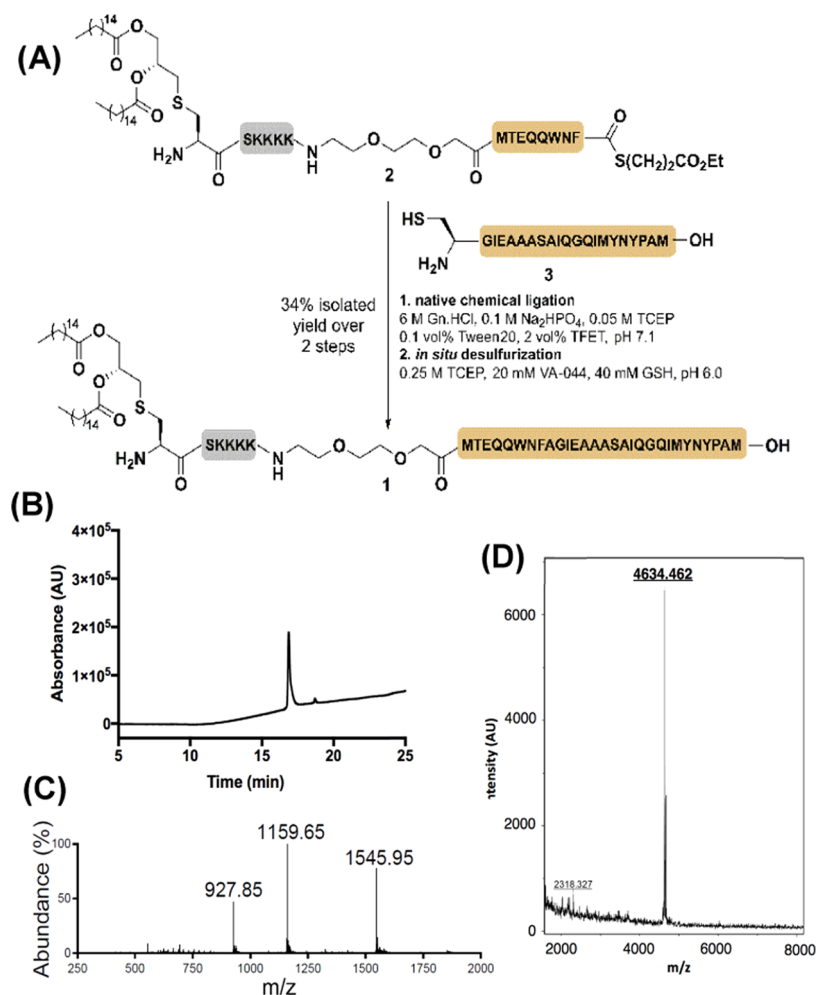
alanine residue at ligation junction) in a one-pot manner.³³
With this synthetic strategy in mind, we chose to disconnect
the vaccine between Phe8 and Ala9 of the ESAT6 epitope
(Figure 1). This led to two synthetic targets, lipopeptide
thioester **2**, bearing an N-terminal Pam₂Cys residue (Scheme
1B), and peptide **3**, possessing an N-terminal cysteine in place
of native Ala9 in the ESAT6 epitope (Scheme 1C).

Scheme 1. (A) Synthesis of Dipeptide Building Block **4** from Boc-Phe-OH; (B) Synthesis of Lipopeptide Thioester Fragment **2** via Side Chain Anchoring, Fmoc-SPPS and Subsequent On-Resin Thioesterification; NB: Amino Acids within Resin-Bound Peptides Possess Standard Side-Chain-Protecting Groups Used in Fmoc-SPPS; (C) Synthesis of Peptide Fragment **3** via Fmoc-SPPS



Synthesis of lipopeptide thioester **2** was achieved via Fmoc-
strategy SPPS on Rink amide resin using an on-resin
thioesterification procedure.³⁴ Initially, we synthesized Fmoc-
AspPhe-OAlI **4** (Scheme 1A). This began by allyl ester
protection of Boc-Phe-OH (**5**) to afford **6**, followed by Boc
deprotection and coupling to Fmoc-Asp(OtBu)-OH to afford
dipeptide **8** in good yield. Deprotection of the side-chain *t*Bu
ester on the aspartate residue then provided the target
dipeptide **4**. With **4** in hand, it was next loaded via the
condensation of the side-chain carboxylate of the aspartate
residue to Rink amide resin (Scheme 1B). The polypeptide
chain was then elongated using iterative Fmoc-SPPS, with 134

Scheme 2. (A) Synthesis of Self-Adjuvanting Tuberculosis Vaccine Candidate **1** via One-Pot Native Chemical Ligation and Desulfurization; (B) Analytical HPLC Chromatogram, (C) electrospray ionization mass spectrometry (ESI-MS), and (D) matrix-assisted laser desorption/ionization time-of-flight (MALDI-TOF) MS Spectrum of Vaccine **1**



135 amino acid, triethyleneglycolate, and Pam₂Cys couplings
 136 effected with *N,N'*-diisopropylcarbodiimide (DIC) and ethyl
 137 (hydroxyimino)cyanoacetate (Oxyma). At this point, the allyl
 138 ester-protected C-terminus of the peptide was unmasked by
 139 treatment with palladium *tetrakis*-triphenylphosphine and
 140 phenylsilane. Treatment with ethyl 3-mercaptopropionate in
 141 the presence of (benzotriazole-1-yl)oxy-
 142 tripyrrolidinophosphonium hexafluorophosphate (PyBOP)
 143 and *N,N*-diisopropylethylamine at -15°C ^{35,36} led to the
 144 formation of the C-terminal thioester with no detectable
 145 epimerization. Cleavage of the peptide thioester using an acidic
 146 cocktail comprising trifluoroacetic acid (TFA), triisopropylsilane,
 147 and water provided the crude lipopeptide thioester, which
 148 was purified via reverse-phase high-performance liquid
 149 chromatography (HPLC) to afford **2** in 21% yield (over 43
 150 steps calculated from the initial resin loading). Peptide **3** was
 151 also accessed via Fmoc-strategy SPPS and isolated in 32% yield
 152 (over 63 iterative steps based on the initial resin loading)
 153 following reverse-phase HPLC (on C18 stationary phase)
 154 (Scheme 1C).

155 With the two target fragments in hand, our attention turned
 156 to the key ligation–desulfurization assembly of vaccine **1**.
 157 Native chemical ligation is typically carried out in aqueous
 158 phosphate buffer (0.1 M, pH \sim 7) containing tris-

(carboxyethyl)phosphine (TCEP, 50 mM) as a reductant 159
 and guanidine hydrochloride (Gdn.HCl, 6 M) as a denaturing 160
 agent. However, lipopeptide thioester **2** was insoluble in this 161
 buffer system and, as a result, we supplemented the buffer with 162
 the nonionic surfactant Tween-20 (0.5% v/v) as a solubilizing 163
 detergent. Specifically, lipopeptide thioester **2** and peptide **3** 164
 were dissolved in this buffer and 2,2,2-trifluoroethanethiol 165
 (TFET, 2% v/v) was added.³³ Pleasingly, within 2 h, the 166
 reaction proceeded to completion to afford the ligation 167
 product. Without purification, *in situ* desulfurization of the 168
 ligation product was performed through treatment with the 169
 radical initiator 2,2'-azobis[2-(2-imidazolin-2-yl)propane]- 170
 dihydrochloride (VA-044) (20 mM) in the presence of 171
 reduced glutathione (40 mM) and TCEP (250 mM) to 172
 convert the cysteine to a native alanine residue at the ligation 173
 junction. HPLC purification using C18 reverse-phase HPLC 174
 furnished self-adjuvanting TB vaccine candidate **1** in 34% yield 175
 over two steps (Scheme 2). 176 s2

The adjuvant activity of the synthesized conjugate vaccine **1** 177
 was first verified *in vitro*. Specifically, Pam₂Cys binding and 178
 activation of the TLR2 signaling pathway was assessed in a 179
 HEK-TLR2-reporter cell line. Conjugate vaccine **1** showed a 180
 strong activation of TLR2, comparable to stimulation with 181
 Pam₂Cys-SKKKK-PEG(OH) (Figure 2). The *in vivo* 182 f2

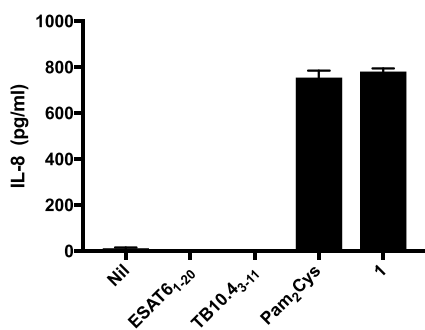


Figure 2. Vaccine candidate **1** activates TLR2 signaling in vitro. Stimulation of IL-8 released from HEK-TLR2 reporter cells by synthetic conjugate **1** is shown in comparison to stimulation with PBS (Nil), ESAT6_{1–20} or TB10.4_{3–11} peptides, or Pam₂Cys-PEG(OH) alone (at ~7 μ M). Data are mean \pm standard error of the mean (SEM) ($n = 3$) and are representative of two independent experiments.

induced substantial populations of ESAT6-specific CD4⁺ T-lymphocytes in the lungs producing IL-17 and TNF α (Figure 3A). The multifunctionality of local T-lymphocytes were also increased, such that significant populations of IL-17⁺ CD4⁺ cells were observed that also expressed other key cytokines, including IFN γ , IL-2, and TNF α , indicative of a predominantly Th17-like phenotype (Figure S1). Notably, there was minimal detectable cytokine response in the lungs of mice that were vaccinated s.c. (Figures 3A and S1). The profile of cytokine-producing ESAT6-specific CD4⁺ T-lymphocytes in the spleens of mucosally immunized mice was similar to that seen in the lungs, but additionally with enhanced IL-2 responses (Figures 3B and S2). A minor population of IL-2- and TNF α -producing cells were observed in the spleens of s.c. immunized mice; however, no other significant populations were identified (Figures 3B and S2). No significant cytokine-producing CD8⁺ populations were seen in the lungs of any immunized group in response to TB10.4_{3–11} (Figure S3A), but small populations of IFN γ - and TNF α -producing CD8⁺ cells were seen in the spleens of s.c. immunized mice (Figure S3B). This may indicate that murine leukocytes were not able to efficiently process this epitope from **1** appropriately for presentation to CD8⁺ T-lymphocytes. Overall, mucosal delivery of the vaccine candidate **1** substantially improved pulmonary immunogenicity and preferentially led to a strong Th17-like CD4⁺ T-lymphocyte response.

Adjuvants for new vaccines should ideally be selected based on their ability to induce the type of immune response best correlated with protection against the pathogen. In the case of Mtb, there is strong evidence that a Th1-type CD4⁺ T-lymphocyte response is required; however, this is not sufficient

immunogenicity induced by **1** was assessed in mice; three homologous vaccinations were given 2 weeks apart and responses were assessed 3 weeks after the final vaccination. Mice were immunized at either the pulmonary mucosa via intranasal (i.n.) instillation or peripherally by subcutaneous (s.c.) injection. The use of defined immunodominant peptide epitopes as antigens enabled quantitative and qualitative assessment of the CD4⁺ and CD8⁺ T-lymphocyte responses generated both locally and systemically. Lymphocytes from the lungs and spleens of immunized mice were restimulated with ESAT6_{1–20} or TB10.4_{3–11} peptides ex vivo prior to intracellular immunostaining and flow cytometry. Mucosal delivery of **1**

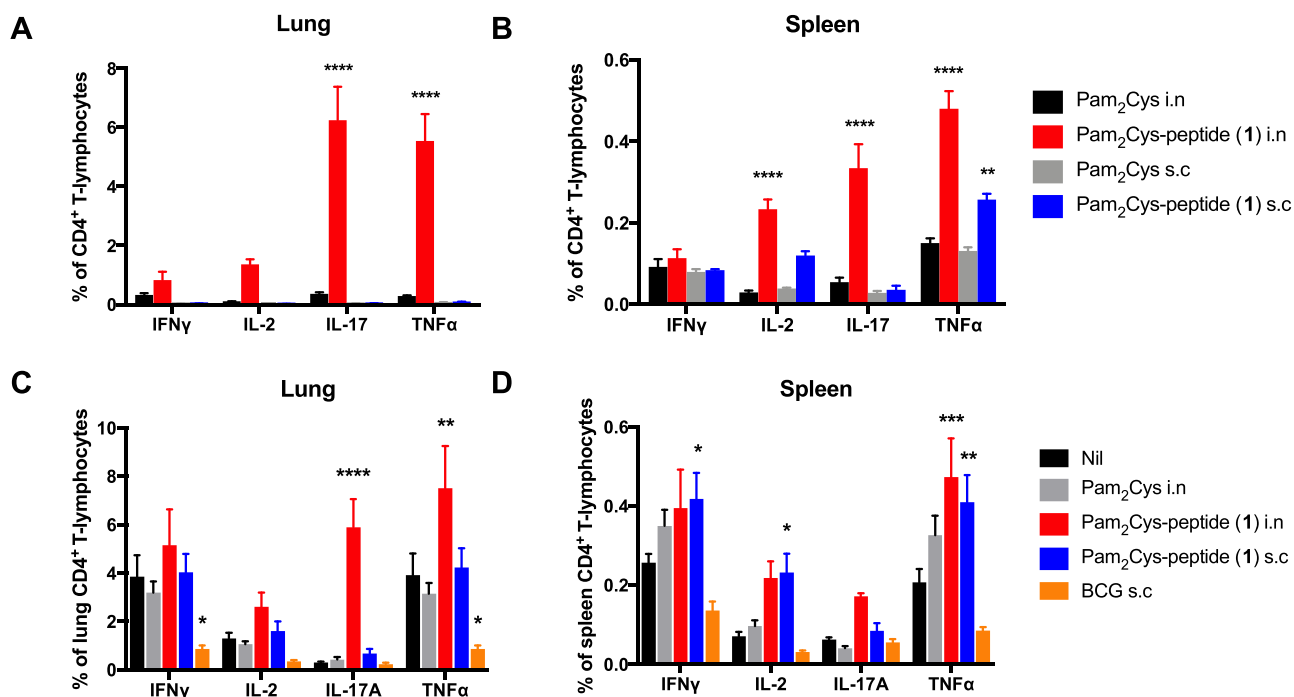


Figure 3. Mucosal, but not peripheral, delivery of **1** induces a strong antigen-specific pulmonary IL-17 and TNF α responses that are maintained post-Mtb challenge. Frequency of cytokine-producing CD4⁺ T-lymphocytes in the (A) lungs and (B) spleen 3 weeks following final immunization ($n = 3$) and (C) lungs and (D) spleen 4 weeks post-Mtb challenge ($n = 6$). Epitope-specific cells were detected by intracellular immunostaining and flow cytometry after recall with ESAT6_{1–20} (10 μ g/mL). Data are mean \pm SEM. Statistically significant differences (A, B) to relevant Pam₂Cys control by analysis of variance (ANOVA) with Tukey's multiple comparison test, and (C, D) to Nil control, by ANOVA with Dunnett's multiple comparison test (* $p < 0.05$, ** $p < 0.01$, *** $p < 0.001$, **** $p < 0.0001$).

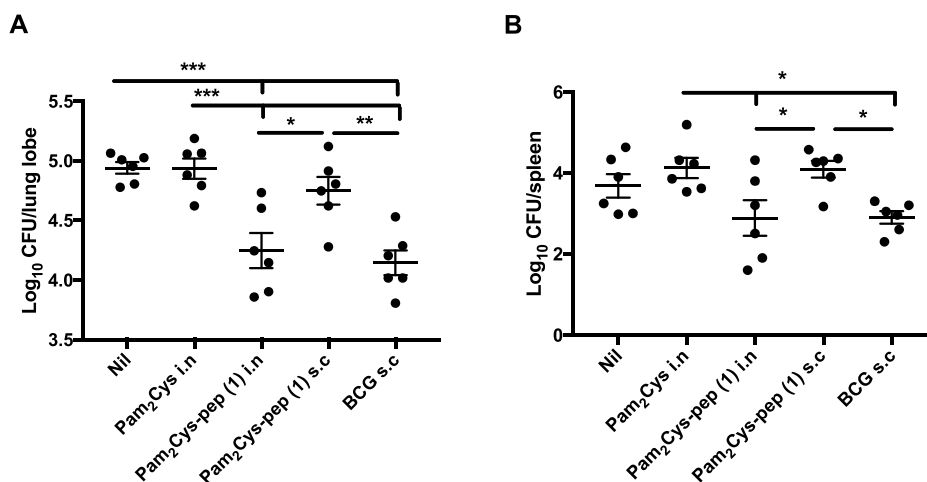


Figure 4. Protective efficacy against Mtb infection was induced by mucosal immunization with **1**. Mice ($n = 6$) were immunized with **1** ($10 \mu\text{g}$ peptide component), or an equivalent amount of Pam₂Cys, three times at two-weekly intervals. Six weeks later, the mice were challenged with aerosol Mtb H37Rv (100 CFU). Alternatively, the mice received $5 \times 10^5 \text{ CFU}$ BCG s.c. 10 weeks before challenge. After 28 days, the bacterial loads in (A) lungs and (B) spleen were enumerated. Data are mean \pm SEM and are representative of two independent experiments. Statistical significance was determined by ANOVA with Tukey's multiple comparisons test (* $p < 0.05$, ** $p < 0.01$, *** $p < 0.001$).

for sterilizing immunity.³⁷ Immunization at the pulmonary mucosa tends to drive a Th17-based response to peptide antigens, likely due to the induction of IL-1, IL-6, and TGF β expression.^{38,39} TLR2 stimulation, which leads to the production of TNF and IL-6, is critical for the activation of antigen-presenting cells²⁸ and are also inducers of Th17 polarization, characterized by IL-17, IL-21, and IL-22 production. IL-17 may promote granuloma formation and neutrophil recruitment by inducing the pro-inflammatory cytokines and chemokines G-CSF, IL-6, and IL-8,^{40,41} as well as recruitment of IFN γ -producing cells to the site of infection by induction of CXCL10 expression.⁴² This is suggested to be one of the mechanisms by which Th17 cells may promote the immune response to Mtb.⁴³ While the role of vaccine-induced IL-17 in protection against Mtb is controversial,^{44,45} several studies have indicated the plasticity of vaccine-induced Th17 cells in mice, and their capacity to revert after exposure to Mtb to expression of the classical Th1-associated cytokine IFN γ , even after long-term residency as memory cells in the lungs.^{46,47} It is therefore possible that mucosal immunization with **1**, despite inducing primarily strong Th17 responses, may provide a pool of lung resident CD4⁺ T-lymphocytes that can function as Th1 or Th17 as needed and provide protective responses against the pathogen.^{12,13}

Having demonstrated robust pulmonary immunogenicity from mucosal administration of **1**, we next tested the self-adjuvanting vaccine candidate in an aerosol Mtb infection. C57BL/6 mice received three homologous immunizations 3 weeks apart with i.n. Pam₂Cys alone or **1** by i.n. instillation or s.c. injection. A separate group of mice received BCG s.c., considered the gold-standard comparison in murine models of Mtb challenge.⁴⁸ After 6 weeks, the mice were challenged by aerosol with Mtb and the postchallenge immune response to the vaccine epitopes were assessed 4 weeks later. Mice immunized i.n. with **1** had maintained significantly upregulated populations of ESAT6-specific CD4⁺ T-lymphocytes producing IL-17 and TNF α in the lungs, which were not seen in peripherally immunized mice (Figure 3C). The diversity of multifunctional cytokine-producing populations in the lungs of mucosally immunized mice was maintained postchallenge

(Figure S4). Populations of a similar phenotype were also seen in the spleen (Figures 3D and S5), consistent with the immunogenicity pre-Mtb challenge. At this postchallenge stage, mice immunized s.c. had increased ESAT6-specific IFN γ ⁺, IL-2⁺, and TNF α ⁺ CD4⁺ T-lymphocyte populations in the spleen (Figures 3D and S5). There were minimal vaccine-induced responses seen to the TB10.4_{3–11} peptide post-challenge, and it is likely that these populations reflect responses to the Mtb challenge itself (Figure S6).

To assess if the T-lymphocyte responses generated by **1** were functionally beneficial, the Mtb bacterial burden in the lungs and spleen were enumerated to determine the protective efficacy of the vaccine. We were pleased to observe that when **1** was delivered mucosally, it provided substantial protection in both the lungs and spleen, similar to that provided by BCG (Figure 4). Consistent with the immunological data, while there was a trend toward protection in the lungs after subcutaneous vaccination, this did not reach statistical significance in all experiments (Figure 4A) and no protection was seen in the spleen (Figure 4B). These data strongly support the model that vaccination strategies promoting a pulmonary immune response offer more robust protection from Mtb. Taken together, this study provides an exciting proof of principle data that synthetic self-adjuvanting peptide vaccines can provide substantial pulmonary immunogenicity and protection against virulent Mtb.

CONCLUSIONS

In summary, we have successfully produced a synthetic lipopeptide conjugate vaccine candidate **1** by one-pot native chemical ligation–desulfurization chemistry and assessed the delivery by pulmonary or peripheral routes to induce protective immune responses to Mtb. Mucosal delivery offered increased immunogenicity and protective efficacy. The use of this vaccine in humans will depend on future toxicology and careful evaluation of the adjuvant Pam₂Cys in phase I clinical studies. It will be important in future studies to assess whether pulmonary vaccination with constructs such as **1** may be used to boost the protective efficacy of BCG or improve the long-term protective efficacy against Mtb. Pulmonary boosting may

have the additional benefit of drawing memory T-lymphocytes generated by subcutaneous BCG into the lungs, creating a further reservoir of memory cells that may act quickly to combat future encounter with Mtb. Further, these conjugated lipopeptides provide the means to assess the impact that the type of conjugation between antigen and adjuvant has on immunogenicity and protective efficacy. The ligation technology employed in this study is applicable to the conjugation of diverse peptide or protein antigens to different adjuvants that stimulate a variety of pattern recognition receptors. Exploring pulmonary administration to enhance efficacy and ease of delivery with a range of different adjuvants and antigens from Mtb may contribute novel constructs to the TB vaccine pipeline and will be the subject of continued work in our laboratories.

EXPERIMENTAL SECTION

General Methods. Unless otherwise stated, reactions were carried out under an argon atmosphere and at room temperature (rt) (22 °C). Reactions carried out at 0 °C employed a bath of water and ice. Anhydrous CH_2Cl_2 and dimethylformamide (DMF) was obtained using a PureSolv solvent purification system (water < 10 ppm). Reactions were monitored by thin layer chromatography (TLC) on aluminum-backed silica plates (Merck Silica Gel 60 F254). Visualization of TLC plates was undertaken with an ultraviolet light at $\lambda = 254$ nm and staining with solutions of vanillin or phosphomolybdic acid, followed by exposure of the stained plates to heat. Silica gel 60 40–63 μm was used for flash column chromatography. NMR spectroscopy was performed in CDCl_3 on a Bruker DRX 300 or DRX 400 NMR spectrometer at frequencies of 300 MHz or 400 MHz for ^1H NMR and 75 or 100 MHz for ^{13}C NMR, respectively. Chemical shifts are reported in parts per million (ppm) and coupling constants in Hertz (Hz). Residual solvent was used as internal standards (CDCl_3 : $\delta_{\text{H}} = 7.26$, $\delta_{\text{C}} = 77.16$). ^{13}C NMR data are reported as chemical shift values (ppm). Mass spectrometry with electrospray ionization (ESI) was performed on a Shimadzu 2020 (ESI) mass spectrometer operating in a positive mode. High-resolution mass spectra were recorded on a Bruker-Daltonics Apex Ultra 7.0T Fourier transform (FTICR) mass spectrometer. MALDI-TOF mass spectrometry was performed on a Bruker Autoflex Speed MALDI-TOF mass spectrometer operating in reflectron mode using a matrix of 10 mg/mL α -cyano-4-hydroxycinnamic acid in water/ acetonitrile containing 0.1% TFA (1:1 v/v). Optical rotations were measured on a PerkinElmer 341 polarimeter at a wavelength of 589 nm. IR spectra were recorded on a Bruker Alpha FT-IR spectrometer using a diamond ATR unit. The purity of all compounds was >97% as judged by NMR spectroscopy and HPLC.

General Procedure for Fmoc-SPPS. Fmoc-SPPS was performed on a Biotage Initiator+ Alstra microwave peptide synthesizer using the following conditions. Amino acid coupling: A solution of Fmoc-protected amino acid (4 equiv), DIC (4 equiv), and Oxyma (4 equiv) in DMF (Labscan, final amino acid concentration 0.1 M) was added to the resin. After 30 min at 50 °C, the resin was washed with DMF (5 \times 5 mL). Deprotection: The resin was treated with 20% piperidine/DMF (2 \times 3 mL, 3 min) at rt and then washed with DMF (5 \times 5 mL). Capping: Ac_2O /pyridine (1:9 v/v) was added to the resin (3 mL). After 3 min, the resin was washed with DMF (5 \times 5 mL).

General Procedure for Resin Cleavage. Peptides were cleaved from resin (with concomitant side-chain deprotection) by treatment with an acidic cocktail containing TFA/triisopropylsilane/water (90:5:5 v/v/v) with gentle shaking for 2 h. The cleavage solution was filtered and the resin washed with TFA (2 \times 2 mL). The solution was concentrated and then precipitated with cold diethyl ether. The mixture was centrifuged and the supernatant was discarded.

Preparative and Semipreparative Reverse-Phase HPLC. HPLC purification was performed using a Waters 600 Multisolvant Delivery System and Waters 500 pump with a Waters 490E

programmable wavelength detector operating at 214, 230, or 280 nm. Peptide 3 was purified by preparative HPLC on a Waters Sunfire C18 column (5 μm , 19 \times 150 mm) at a flow rate of 7 mL min^{-1} (solvent A: 0.1% TFA in H_2O ; solvent B: 0.1% TFA in MeCN). Lipopeptides 1 and 2 were purified by semipreparative HPLC on a Phenomenex Luna C18(2) column (5 μm , 10 \times 250 mm) in a column heater at 40 °C and a flow rate of 7 mL min^{-1} (solvent A: 0.1% TFA in H_2O :MeCN:iPrOH (8:1:1 v/v/v); solvent B: 0.1% TFA in MeCN:iPrOH (9:1 v/v/v)).

Synthesis of Vaccine 1 via One-Pot Native Chemical Ligation Desulfurization. Lipopeptide thioester 2 (2.5 mg, 0.96 μmol) and peptide 3 (2 equiv, 4.2 mg, 1.92 μmol) were dissolved in aqueous phosphate buffer (0.1 M, pH = 7.4, 192 μL , 5 mM with respect to thioester 2) containing guanidine hydrochloride (6 M), TCEP (50 mM), and Tween-20 (0.5% v/v). The pH of the reaction mixture was adjusted with aqueous NaOH (1 M) to pH 7.2. TFET (2% v/v) was added and the reaction was incubated at 37 °C for 2 h. The reaction was followed by ultraperformance liquid chromatography-tandem mass spectrometry (UPLC-MS). After consumption of the thioester (as measured by UPLC-MS analysis, 2 h) the reaction was degassed under a stream of argon, and one volume of degassed aqueous phosphate buffer containing guanidine hydrochloride (6 M), TCEP (500 mM), reduced glutathione (80 mM), and the radical initiator VA-044 (40 mM) was added. The reaction was allowed to proceed at 37 °C for 8 h, at which time the ligation product bearing cysteine at the ligation junction was fully converted to the corresponding alanine-containing product (as judged by UPLC-MS analysis). Semipreparative HPLC purification (0–60% B over 40 min, 7 mL min^{-1} , 40 °C, Phenomenex Luna C18(2), 5 μm , 100 \AA , 10 \times 250 mm) followed by lyophilization afforded pure vaccine candidate 1 as a white solid (1.5 mg, 34% yield). Analytical HPLC: R_t 16.9 min symmetry C4 column, 300 \AA , 5 μm , 4.6 mm \times 250 mm, gradient: 20–100 B over 25 min (solvent A: H_2O + 0.1% TFA, solvent B: MeCN + 0.1% TFA); MS calcd: $[\text{M} + 3\text{H}]^{3+} = 1545.48$, $[\text{M} + 4\text{H}]^{4+} = 1159.36$, $[\text{M} + 5\text{H}]^{5+} = 927.69$; found (ESI $^{+}$): 1545.95, 1159.65, 927.85. HRMS calcd for $\text{C}_{214}\text{H}_{348}\text{N}_{47}\text{O}_{58}\text{S}_4$: $[\text{M} + \text{H}]^{+} = 4634.466$; found (MALDI-TOF): 4634.462.

Synthesis of Lipopeptide Thioester 2. Rink amide resin (25 μmol , 0.3 mmol/g loading) was initially washed with CH_2Cl_2 (5 \times 3 mL) and DMF (5 \times 3 mL), followed by Fmoc deprotection with 20% piperidine/DMF (2 \times 5 min). The resin was washed with DMF (5 \times 3 mL), CH_2Cl_2 (5 \times 3 mL), and DMF (5 \times 3 mL). PyBOP (4 equiv) and *N*-methylmorpholine (NMM) (8 equiv) were added to a solution of Fmoc-AspPhe-OAll 4 (4 equiv) in DMF. After 5 min of preactivation, the mixture was added to the resin and then shaken at rt for 2 h. The resin was filtered, then washed with DMF (5 \times 3 mL), CH_2Cl_2 (5 \times 3 mL), and DMF (5 \times 3 mL), capped with Ac_2O /pyridine (1:9 v/v; 2 \times 3 min), and washed with DMF (5 \times 3 mL), CH_2Cl_2 (5 \times 3 mL), and DMF (5 \times 3 mL). The resin-bound H-SKKKK-triethyleneglycolate-ESAT6(1–8) peptide was synthesized on the side-chain-loaded resin using the general procedure for Fmoc-SPPS. For the coupling of Pam $_2$ Cys, a solution of Fmoc-Pam $_2$ Cys-OH (1.2 equiv), DIC (1.2 equiv), and HOAt (1.5 equiv) in DMF was added to the resin, and the reaction was shaken at rt for 16 h. The resin was next treated with a solution of $\text{Pd}(\text{PPh}_3)_4$ (1 equiv) and PhSiH_3 (40 equiv) in dry CH_2Cl_2 . The resin was shaken for 1 h and the procedure was repeated. Afterward, the resin was washed with CH_2Cl_2 (10 \times 5 mL), DMF (5 \times 5 mL), and CH_2Cl_2 (5 \times 5 mL). A solution of ethyl-3-mercaptopropionate (4 equiv) and PyBOP (4 equiv) in DMF (2–3 mL) was added to the resin at –15 °C in a salt-ice-water bath. Subsequently, $^i\text{Pr}_2\text{NEt}$ (4 equiv) was added to the resin. The resin was left at –15 °C for 3 h. Afterward, the resin was washed with CH_2Cl_2 (10 \times 5 mL), DMF (5 \times 5 mL), and CH_2Cl_2 (5 \times 5 mL). The peptide was cleaved from resin and worked up as described in the general resin cleavage procedure. The dried pellet was dissolved in water containing 40% MeCN + 0.1% TFA, purified by preparative RP-HPLC (50–100% B over 40 min, 4 mL min^{-1} , 40 °C, Phenomenex Luna C18(2), 5 μm , 100 \AA , 10 \times 250 mm) and lyophilized to afford the desired lipopeptide thioester as a white solid (13.5 mg, 21% yield). Analytical HPLC: R_t 16.0 min (50–100% B 441

442 over 30 min, 0.2 mL min⁻¹, Phenomenex Luna C18(2), 5 μ m, 2.1 \times
443 150 mm, λ = 214 nm). MS calcd: [M + 2H]²⁺ = 1300.24, [M + 3H]³⁺
444 = 867.17, [M + 4H]⁴⁺ = 650.62; found (ESI⁺): 1300.80, 867.45,
445 650.75.

446 **Synthesis of Peptide 3.** 2-Chlorotrityl chloride resin (50 μ mol,
447 1.22 mmol/g loading) was swollen in dry CH₂Cl₂ for 30 min then
448 washed with CH₂Cl₂ (5 \times 3 mL). A solution of Fmoc-Met-OH (0.5
449 equiv relative to resin functionalization) and ⁱPr₂NEt (2.0 equiv
450 relative to resin functionalization) in CH₂Cl₂ (final amino acid
451 concentration 0.1 M of amino acid) was added and the resin was
452 shaken at rt for 16 h. The resin was washed with DMF (5 \times 3 mL)
453 and CH₂Cl₂ (5 \times 3 mL). The resin was treated with a solution of
454 CH₂Cl₂/CH₃OH/ⁱPr₂NEt (17:2:1 v/v/v, 3 mL) for 1 h and washed
455 with DMF (5 \times 3 mL), CH₂Cl₂ (5 \times 3 mL), and DMF (5 \times 3 mL).
456 The ESAT6(9–20)-TB10.4(3–11) peptide was synthesized via
457 Fmoc-strategy solid-phase peptide synthesis as outlined in the general
458 methods section. The peptide was cleaved from resin and worked up
459 via the general resin cleavage procedure. The dried pellet was
460 dissolved in water containing 30% MeCN + 0.1% TFA and purified by
461 preparative HPLC (0–60% B over 40 min, 7 mL min⁻¹, Sunfire C18,
462 5 μ m, 100 Å, 19 \times 150 mm) to afford the desired peptide as a white
463 solid (35 mg, 32% yield). Analytical HPLC: R_t 13.1 min (0–100% B
464 over 30 min, 0.2 mL min⁻¹, 0.1% TFA, Sunfire C18, 5 μ m, 100 Å, 2.1
465 \times 150 mm, λ = 214 nm). MS calcd: [M + 2H]²⁺ = 1102.50, [M +
466 3H]³⁺ = 735.33; found (ESI⁺): 1102.60, 734.45.

467 **Fmoc-L-Asp-L-Phe-OAll (4).** The protected dipeptide **8** (872 mg,
468 1.42 mmol) was treated with TFA in CH₂Cl₂ (10 mL, 1:1 v/v). The
469 reaction mixture was stirred at room temperature for 1 h, after which
470 the TFA/CH₂Cl₂ solvent mixture was removed under a gentle stream
471 of nitrogen. The residue was dissolved in CH₂Cl₂ and then washed
472 with water (2 \times 30 mL), saturated aqueous NaHCO₃ solution (2 \times
473 30 mL), and brine (30 mL). The organic phase was dried with
474 anhydrous MgSO₄, concentrated in vacuo, and purified by flash
475 column chromatography to afford the target compound **4** as a yellow
476 oil (728 mg, 90% yield). R_f = 0.42 (EtOAc/hexane: 1:2 v/v) ¹H NMR
477 (CDCl₃, 400 MHz) δ (ppm): 7.77 (d, J = 7.4 Hz, 2H), 7.54 (m,
478 2H), 7.39 (t, J = 7.4 Hz, 2H), 7.29 (t, J = 7.4 Hz, 2H), 7.20–7.08 (m,
479 6H), 5.97 (d, 8.1 Hz, 1H), 5.82 (ddt, J = 5.5, 10.5, 16.5 Hz, 1H), 5.25
480 (dd, J = 17.9, 10.5 Hz, 2H), 4.85 (dd, 6.3, 6.8 Hz, 1H), 4.56 (m, 3H),
481 4.42–4.34 (m, 2H), 4.18 (t, J = 7.0 Hz, 1H), 3.12–3.06 (m, 3H),
482 2.70 (m, 1H); ¹³C NMR (CDCl₃, 100 MHz) δ (ppm): 170.8, 156.1,
483 143.6, 141.3, 141.2, 135.5, 131.2, 129.2, 128.5, 128.5, 127.8, 127.2,
484 127.1, 125.1, 120.0, 119.1, 67.5, 66.2, 53.6, 50.7, 47.0, 37.7, 35.9;
485 HRMS: (+ESI) Calc. for 542.2053 [M + Na]⁺, found: 542.2058 [M +
486 Na]⁺; IR (ATR): ν_{max} = 3300, 3065, 3030, 2924, 2854, 1710, 1661,
487 1532, 1449, 1248, 1211, 1049, 738, 701 cm⁻¹; [α]_D: +21° (c 1.0,
488 CH₂Cl₂).

489 **Boc-L-Phe-OAll (6).** Boc-L-Phe-OH **5** (799 mg, 3.0 mmol) was
490 dissolved in DMF (10 mL) and cooled to 0 °C in an ice bath. ⁱPr₂NEt
491 (1.57 mL, 9 mmol) was added dropwise, followed by allyl bromide
492 (280 μ L, 3.3 mmol). The solution was allowed to warm to rt and
493 stirred for 16 h. The reaction mixture was diluted with EtOAc (40
494 mL), and then washed with water (2 \times 30 mL) and brine (30 mL).
495 The organic phase was dried with anhydrous MgSO₄, concentrated in
496 vacuo, and purified via flash column chromatography to afford allyl
497 ester **6** as a yellow oil (905 mg, 99% yield). ¹H NMR (CDCl₃, 400
498 MHz) δ (ppm): 7.33–7.13 (m, 5H), 5.88 (ddt, J = 5.7, 11.0, 16.2 Hz,
499 1H), 5.32 (dq, J = 2.0, 17.3 Hz, 1H), 5.26 (dd, J = 2.0, 10.5 Hz, 1H),
500 4.62 (dt, J = 1.5, 6.0 Hz, 2H), 3.18–3.05 (m, 2H), 1.44 (s, 9H). ¹³C
501 NMR (CDCl₃, 100 MHz) δ (ppm): 171.6, 155.1, 135.9, 131.5, 129.4,
502 128.5, 127.2, 118.9, 79.9, 65.9, 54.5, 38.4, 28.3. These data are in
503 agreement with those previously reported by Lang et al.⁴⁹

504 **L-Phe-OAll (7).** Boc-L-Phe-OAll (**6**) (885 mg, 2.90 mmol) was
505 treated with TFA in CH₂Cl₂ (10 mL, 1:1 v/v). The reaction mixture
506 was stirred at room temperature for 1 h, after which the TFA/CH₂Cl₂
507 solvent mixture was removed under a gentle stream of nitrogen. The
508 reaction mixture was diluted into CH₂Cl₂ (30 mL) and then washed
509 with water (2 \times 30 mL) and brine (30 mL). The organic phase was
510 dried with anhydrous MgSO₄ and then concentrated in vacuo to
511 afford **7** as a yellow oil (592 mg, 99% yield). ¹H NMR (CDCl₃, 400

MHz) δ (ppm): 7.27–7.07 (m, 5H), 5.70 (ddt, J = 5.7, 11.0, 16.2 Hz, 1H),
5.20–5.16 (m, 2H), 4.49 (d, J = 6.1 Hz, 2H), 4.20 (t, J = 7.0 Hz, 1H),
3.24–3.11 (m, 2H); ¹³C NMR (CDCl₃, 100 MHz) δ (ppm): 168.6, 132.9,
130.2, 129.3, 128.2, 120.2, 67.4, 54.3, 36.2. These data are in agreement
515 with those previously reported by Lang et al.⁴⁹

516 **Fmoc-L-Asp(OrBu)-L-Phe-OAll (8).** A solution of Fmoc-L-Asp-
517 (OrBu)-OH (1.21 g, 2.91 mmol), HATU (1.11 mg, 2.90 mmol), and
518 N-methylmorpholine (NMM, 1 mL, 9.0 mmol) in DMF (final amino
519 acid concentration 0.1 M) was added to a reaction vessel containing
520 H-L-Phe-OAll **7** (533 mg, 2.6 mmol). The reaction was stirred for 2 h,
521 after which the solvent was removed under a stream of nitrogen. The
522 residue was dissolved into CH₂Cl₂ (30 mL), washed with water (2 \times
523 30 mL), 2 M HCl (20 mL), saturated aqueous NaHCO₃ solution (20
524 mL), and brine (30 mL). The organic phase was dried with anhydrous
525 MgSO₄, concentrated in vacuo, and purified by flash column
526 chromatography to afford the target compound **8** as a yellow oil
527 (1.14 g, 74% yield); R_f = 0.40 (EtOAc/hexane, 3:7 v/v). ¹H NMR
528 (CDCl₃, 300 MHz) δ (ppm): 7.72 (d, J = 7.9 Hz, 2H), 7.53 (d, J =
529 7.5 Hz, 2H), 7.36 (dd, J = 7.1, 7.4 Hz, 2H), 7.30–6.96 (m, 7H), 5.90
530 (d, J = 7.6 Hz, 1H), 5.79 (ddt, J = 6.0, 11.2, 16 Hz, 1H), 5.22 (d, J =
531 18, 10.6 Hz, 2H), 4.80 (dd, J = 13.1, 6.2 Hz, 1H), 4.50 (m, 1H),
532 4.37–4.27 (m, 2H), 4.17 (dd, J = 14.1, 7.1 Hz, 1H), 3.07 (dd, J = 6.2,
533 5.7 Hz, 2H), 2.84 (dd, 17, 4.0 Hz, 1H), 2.56 (dd, 17, 6.6 Hz, 1H),
534 1.40 (s, 9H); ¹³C NMR (CDCl₃, 75 MHz) δ (ppm): 171.2, 170.6,
535 170.2, 155.9, 143.7, 141.3, 135.6, 131.4, 129.3, 128.5, 127.7, 127.1,
536 125.1, 120.0, 119.0, 81.9, 67.3, 66.0, 53.6, 50.9, 47.0, 37.8, 28.5;
537 HRMS: (+ESI) Calc. for 598.2679 [M + Na]⁺, found: 598.2681 [M +
538 Na]⁺; IR (ATR): ν_{max} = 3301, 3066, 3030, 2924, 2854, 1711, 1661,
539 1532, 1449, 1248, 1211, 1050, 738, 701 cm⁻¹; [α]_D: +6.25° (c 1.0,
540 CH₂Cl₂).

541 **In Vitro Assessment of Vaccine Adjuvant Activity.** Human
542 Embryonic Kidney 293 (HEK293; ATCC CRL-1573) cells, stably
543 transfected with a plasmid expressing YFP-TLR2 fusion protein⁵⁰ that
544 secretes IL-8 upon TLR activation (kindly provided by A/Prof Ashley
545 Mansell, Monash University), were used as a reporter of TLR2
546 stimulation by Pam₂Cys in the vaccine construct. Cells were grown in
547 Dulbecco's modified Eagle's medium (Gibco, MA) with D-glucose
548 (4.5 g/L), L-glutamine (3.996 mM), penicillin–streptomycin (100 U/
549 mL; Gibco), geneticin (0.5 mg/mL; Gibco), and 10% heat-inactivated
550 fetal calf serum (FCS) at 37 °C and 5% CO₂. After seeding 2 \times 10⁵
551 cells/well of a 96-well flat-bottom plate (Corning) and allowing cells
552 to adhere, the cells were stimulated in triplicate for 16–18 h with
553 vaccine candidate **1** (33.5 μ g/mL; such that Pam₂Cys-SKKKK-
554 triethyleneglycolate was at 10 μ g/mL, the optimal concentration for
555 stimulation of this cell line as determined by previous experiments,
556 ESAT6_{1–20} ~15 μ g/mL and TB10.4_{3–11} ~8 μ g/mL). As a
557 comparison, Pam₂Cys-SKKKK-triethyleneglycolate (10 μ g/mL),
558 ESAT6_{1–20} peptide (15 μ g/mL), or TB10.4_{3–11} peptide (Genscript;
559 8 μ g/mL) was also used as a stimulus. Supernatants were collected
560 and IL-8 secretion determined as a measure of stimulation of TLR2
561 by ELISA (Biolegend), according to manufacturer's instructions. Data
562 shown are representative of two independent experiments.

563 **Mice and Immunization Procedures.** All murine experiments
564 were conducted with the approval of the Sydney Local Health District
565 Animal Welfare Committee (protocol numbers 2013/054, 2013/075,
566 and 2016/044), in full compliance with local and institutional
567 guidelines. Female C57BL/6 6- to 8-week old mice were obtained
568 from Animal BioResources (Moss Vale, NSW, Australia). The mice
569 were housed in the Centenary Institute animal facility under SPF
570 conditions. For i.n. administration, mice were anesthetized by
571 intraperitoneal injection of ketamine/xylazine solution (50 mg/6.25
572 mg/kg). Vaccine (14.2 μ g, equivalent to 10 μ g peptide) in phosphate-
573 buffered saline (PBS; 50 μ L final volume, such that the vaccine
574 reached the deep lung) was applied to the nares and mice allowed to
575 inhale the solution. Mice receiving subcutaneous vaccines (14.2 μ g for
576 protection studies and 56.8 μ g for immunogenicity studies, equivalent
577 to 10 or 40 μ g peptide respectively; in PBS, 200 μ L final volume)
578 were anesthetized with gaseous isoflurane (4%) and injected at the
579 base of tail. No adverse effects were observed in mice receiving this
580 vaccine by either mucosal or subcutaneous routes. Mice received 3
581

582 vaccinations 2 weeks apart and proceeded to either immunogenicity
583 study at 3 weeks after last vaccination, or Mtb challenge at 6 weeks
584 after last vaccination. Mice receiving BCG were vaccinated s.c. once
585 only with 5×10^5 CFU, 10 weeks prior to Mtb challenge.

586 **Bacterial Strains and Growth Conditions.** *Mangora bovis* BCG
587 Pasteur 1173P2 and Mtb H37Rv (BEI Resources, NIAID, NIH, NR-
588 13648) were cultured at 37 °C in Middlebrook 7H9 (Difco) broth
589 supplemented with albumin-dextrose-catalase (ADC; 10% v/v),
590 Tween-80 (0.05% v/v), and glycerol (0.2% v/v). To enumerate,
591 cultures were plated onto Middlebrook 7H10 or 7H11 (Difco) agar,
592 supplemented with oleic-acid-albumin-dextrose catalase (10% v/v)
593 and glycerol (0.5% v/v) and incubated at 37 °C for up to 21 days.

594 **Experimental Mtb Infection.** At 6 weeks after 3 immunizations,
595 mice received a low-dose aerosol infection (100 CFU) in an
596 inhalation exposure system (Glas-Col, Terre Haute, IN). At 4
597 weeks after challenge, serial dilutions of lung and spleen homogenates
598 were plated to enumerate the bacterial loads.

599 **Collection and Processing of Murine Organs for Leukocyte**
600 **Isolation.** Mice were sacrificed via CO₂ asphyxiation, the tissues
601 removed aseptically and maintained at 4 °C. Circulating blood was
602 removed from the lung lobes by perfusion with an injection of PBS
603 and heparin (20 U/mL; Sigma) into the right atrium of the heart. For
604 isolation of leukocytes, diced tissue was digested with collagenase type
605 4197 (50 U/mL; Sigma) and DNase I (13 µg/mL; Sigma) at 37 °C
606 for 45 min, followed by homogenization and multiple filtration steps
607 through a 70 µm sieve. The spleen, mediastinal lymph node (MLN)
608 of i.n. immunized mice or inguinal lymph nodes (ILN) of s.c.
609 immunized mice was homogenized through a 70 µm sieve and the
610 leukocytes pelleted by centrifugation. Erythrocytes were removed by
611 ACK lysis buffer, then viable leukocytes enumerated by hemocytometer
612 or using a BD Countess, with Trypan Blue (0.04%) exclusion.

613 **Polyfunctional T-Lymphocyte Responses to Immunization.**
614 Epitope-specific cytokine production by T-lymphocytes was enumerated
615 by antigen-recall, intracellular immunostaining, and flow
616 cytometry. Single-cell suspensions of up to 4×10^6 lymphocytes
617 were stimulated for 1–2 h (37 °C, 5% CO₂) with ESAT6_{1–20} or
618 TB10.4_{3–11} peptides (10 µg/mL; Genscript), or with antimouse CD3
619 (1452C11, 5 µg/mL) and antimouse CD28 (37.51, 5 µg/mL; BD
620 Pharmingen) or media alone as controls. Brefeldin A (10 µg/mL;
621 Sigma) was added and further incubation (16 h, 37 °C, 5% CO₂)
622 allowed intracellular accumulation of cytokine. After washing with
623 FACS wash (PBS with 2% FCS), Fc receptors were blocked with
624 antimouse CD16/CD32 (2.4G2; BD Biosciences). Surface markers
625 were labeled with an antimouse CD8-APCCy7 (53-6.7; BD
626 Pharmingen, San Jose, CA), CD4-PECy7 (RM4-5; BD Pharmingen),
627 CD3-PerCPCy5.5 (17A2; Biolegend, San Diego, CA), and Live/Dead
628 fixable blue dead cell stain (Invitrogen, CA) in FACS wash, then the
629 cells were washed thoroughly. Cells were fixed using BD Cytofix/
630 perm, followed by thorough washing with BD Perm/Wash. To label
631 intracellular cytokines, cells were incubated with antimouse IFN-
632 FITC (XMG1.2; BD Pharmingen), IL-17A-PB (TC11-18H10.1;
633 Biolegend), TNFα-PE/APC (MP6-XT22; Biolegend), and IL-2-
634 APC/PE (JES6-SH4; Biolegend) prepared in BD Perm/Wash buffer
635 and then washed. Compensation controls were prepared by
636 immunostaining BD CompBeads with the same antibody utilized in
637 the experimental panel, except for live dead staining, in which case
638 murine leukocytes were labeled in the same manner as experimental
639 samples. Immunostained cells or beads were fixed in 10% neutral
640 buffered formalin prior to the acquisition of the data using an
641 LSRFortessa or LSR II SL flow analyser (BD Biosciences) and analysis
642 using FlowJo (Tree Star Inc.).

643 **Statistical Analysis.** Statistical analysis was performed using
644 GraphPad Prism 6 or 7 software (GraphPad Software, La Jolla, CA),
645 as detailed in figure legends. Differences between two groups were
646 analyzed by Student's *t*-test, or between multiple groups by one- or
647 two-way analysis of variance (ANOVA) with Tukey's or Dunnett's
648 multiple comparisons test and were considered significant when *p*
649 values were ≤ 0.05 (**p* < 0.05, ***p* < 0.01, ****p* < 0.001, *****p* <
650 0.0001).

■ ASSOCIATED CONTENT

● Supporting Information

The Supporting Information is available free of charge on the
ACS Publications website at DOI: 10.1021/acs.jmed-
chem.9b00832.

NMR spectra, MALDI-TOF mass spectrum of **1**, and
immunological data (PDF)

Molecular formula strings (CSV)

■ AUTHOR INFORMATION

Corresponding Authors

*E-mail: w.britton@centenary.org.au (W.J.B.).

*E-mail: richard.payne@sydney.edu.au (R.J.P.).

ORCID

Richard J. Payne: 0000-0002-3618-9226

Author Contributions

||A.S.A. and D.M.M. contributed equally to this work.

Author Contributions

All authors have given approval to the final version of the
manuscript.

Funding

This work was supported by the National and Medical
Research Council of Australia Project Grant (APP1044343),
Centre for Research Excellence in Tuberculosis Control
(APP1043225), and the NSW Government through its
infrastructure grant to the Centenary Institute. A.S.A.,
D.M.M., and C.C.H. each received an Australian Postgraduate
Award.

Notes

The authors declare no competing financial interest.

■ ACKNOWLEDGMENTS

We thank Prof J Triccas, the University of Sydney, for
provision of BCG stocks, Dr B Saunders, the University of
Technology Sydney, for provision of antimouse CD3 antibody
and A/Prof A Mansell, Monash University, for provision of
HEK-TLR2 reporter cell line stocks. We thank Dr G
Nagalingam, Dr D Quan, Dr L Lin, Dr M Flórido, and Dr S
Rudrawar, the Centenary Institute Animal Facility and Sydney
Cytometry, for technical assistance and advice.

■ ABBREVIATIONS

BCG, *Mycobacterium bovis* bacille Calmette–Guérin; DIC,
N,N'-diisopropylcarbodiimide; i.n., intranasal; Mtb, *Mycobac-*
terium tuberculosis; Oxyma, ethyl (hydroxyimino)cyanoacetate;
PyBOP, (benzotriazole-1-yloxy)tripyrrolidinophosphonium
hexafluorophosphate; SPPS, solid-phase peptide synthesis;
TCEP, tris(2-carboxyethyl)phosphine hydrochloride; TFET,
2,2,2-trifluoroethanethiol; Th, T-helper; VA-044, 2,2'-azobis-
[2-(2-imidazolin-2-yl)propane]dihydrochloride

■ REFERENCES

- (1) Kaufmann, S. H. E.; Hussey, G.; Lambert, P.-H. New vaccines
for tuberculosis. *Lancet* **2010**, 375, 2110–2119.
- (2) *Global Tuberculosis Report*; World Health Organization: Geneva,
2018.
- (3) Andersen, P.; Doherty, T. M. The success and failure of BCG-
implications for a novel tuberculosis vaccine. *Nat. Rev. Microbiol.*
2005, 3, 656–662.
- (4) Marais, B. J.; Sintchenko, V. Epidemic spread of multidrug-
resistant tuberculosis in China. *Lancet Infect. Dis.* **2017**, 17, 238–239.

- (5) Marais, B. J.; Mlambo, C. K.; Rastogi, N.; Zozio, T.; Duse, A. G.; Victor, T. C.; Marais, E.; Warren, R. M. Epidemic spread of multidrug-resistant tuberculosis in Johannesburg, South Africa. *J. Clin. Microbiol.* **2013**, *51*, 1818–1825.
- (6) Ragonnet, R.; Trauer, J. M.; Denholm, J. T.; Marais, B. J.; McBryde, E. S. High rates of multidrug-resistant and rifampicin-resistant tuberculosis among re-treatment cases: where do they come from? *BMC Infect. Dis.* **2017**, *17*, No. 36.
- (7) Nemes, E.; Geldenhuys, H.; Rozot, V.; Rutkowski, K. T.; Ratangee, F.; Bilek, N.; Mabwe, S.; Makhethe, L.; Erasmus, M.; Toefy, A.; Mulenga, H.; Hanekom, W. A.; Self, S. G.; Bekker, L.-G.; Ryall, R.; Gurunathan, S.; DiazGranados, C. A.; Andersen, P.; Kromann, I.; Evans, T.; Ellis, R. D.; Landry, B.; Hokey, D. A.; Hopkins, R.; Ginsberg, A. M.; Scriba, T. J.; Hatherill, M. Prevention of *M. tuberculosis* infection with H4:IC31 vaccine or BCG revaccination. *N. Engl. J. Med.* **2018**, *379*, 138–149.
- (8) Van Der Meeren, O.; Hatherill, M.; Nduba, V.; Wilkinson, R. J.; Muyoyeta, M.; Van Brakel, E.; Ayles, H. M.; Henostroza, G.; Thienemann, F.; Scriba, T. J.; Diacon, A.; Blatner, G. L.; Demoitié, M.-A.; Tameris, M.; Malahleha, M.; Innes, J. C.; Hellström, E.; Martinson, N.; Singh, T.; Akite, E. J.; Khatoon Azam, A.; Bollaerts, A.; Ginsberg, A. M.; Evans, T. G.; Gillard, P.; Tait, D. R. Phase 2b controlled trial of M72/AS01E vaccine to prevent tuberculosis. *N. Engl. J. Med.* **2018**, *379*, 1621–1634.
- (9) Sabin, A. B. Immunization against measles by aerosol. *Rev. Infect. Dis.* **1983**, *5*, 514–523.
- (10) Saluja, V.; Amorij, J. P.; Kapteyn, J. C.; de Boer, A. H.; Frijlink, H. W.; Hinrichs, W. L. J. A comparison between spray drying and spray freeze drying to produce an influenza subunit vaccine powder for inhalation. *J. Controlled Release* **2010**, *144*, 127–133.
- (11) Cutts, F. T.; Clements, C. J.; Bennett, J. V. Alternative routes of measles immunization: a review. *Biologicals* **1997**, *25*, 323–338.
- (12) Lu, D.; Hickey, A. J. Pulmonary vaccine delivery. *Expert Rev. Vaccines* **2007**, *6*, 213–216.
- (13) Perdomo, C.; Zedler, U.; Köhl, A. A.; Lozza, L.; Saikali, P.; Sander, L. E.; Vogelzang, A.; Kaufmann, S. H. E.; Kupz, A. Mucosal BCG vaccination induces protective lung-resident memory T cell populations against tuberculosis. *mBio* **2016**, *7*, No. e01686-16.
- (14) Tameris, M. D.; Hatherill, M.; Landry, B. S.; Scriba, T. J.; Snowden, M. A.; Lockhart, S.; Shea, J. E.; McClain, J. B.; Hussey, G. D.; Hanekom, W. A.; Mahomed, H.; McShane, H. Safety and efficacy of MVA85A, a new tuberculosis vaccine, in infants previously vaccinated with BCG: a randomised, placebo-controlled phase 2b trial. *Lancet* **2013**, *1*, 60177–60174.
- (15) Satti, I.; Meyer, J.; Harris, S. A.; Thomas, Z.-R. M.; Griffiths, K.; Antrobus, R. D.; Rowland, R.; Ramon, R. L.; Smith, M.; Sheehan, S.; Bettinson, H.; McShane, H. Safety and immunogenicity of a candidate tuberculosis vaccine MVA85A delivered by aerosol in BCG-vaccinated healthy adults: a phase 1, double-blind, randomised controlled trial. *Lancet Infect. Dis.* **2014**, *14*, 939–946.
- (16) White, A. D.; Sibley, L.; Dennis, M. J.; Gooch, K.; Betts, G.; Edwards, N.; Reyes-Sandoval, A.; Carroll, M. W.; Williams, A.; Marsh, P. D.; McShane, H.; Sharpe, S. A. Evaluation of the safety and immunogenicity of a candidate tuberculosis vaccine, MVA85A, delivered by aerosol to the lungs of macaques. *Clin. Vaccine Immunol.* **2013**, *20*, 663–672.
- (17) Kaufmann, S. H. E. Future vaccination strategies against tuberculosis: thinking outside the box. *Immunity* **2010**, *33*, 567–577.
- (18) Parida, S. K.; Kaufmann, S. H. E. Novel tuberculosis vaccines on the horizon. *Curr. Opin. Immunol.* **2010**, *22*, 374–384.
- (19) Ingale, S.; Wolfert, M. A.; Gaekwad, J.; Buskas, T.; Boons, G. J. Robust immune responses elicited by a fully synthetic three-component vaccine. *Nat. Chem. Biol.* **2007**, *3*, 663–667.
- (20) McDonald, D. M.; Wilkinson, B. L.; Corcilius, L.; Thaysen-Andersen, M.; Byrne, S. N.; Payne, R. J. Synthesis and immunological evaluation of self-adjuvanting MUC1-macrophage activating lipopeptide 2 conjugate vaccine candidates. *Chem. Commun.* **2014**, *50*, 10273–10276.
- (21) Moyle, P. M.; Olive, C.; Good, M. F.; Toth, I. Method for the synthesis of highly pure vaccines using the lipid core peptide system. *J. Pept. Sci.* **2006**, *12*, 800–807.
- (22) Wilkinson, B. L.; Day, S.; Malins, L. R.; Apostolopoulos, V.; Payne, R. J. Self-adjuvanting multicomponent cancer vaccine candidates combining per-glycosylated MUC1 glycopeptides and the Toll-like receptor 2 agonist Pam₃CysSer. *Angew. Chem., Int. Ed.* **2011**, *50*, 1635–1639.
- (23) Cai, H.; Chen, M.-S.; Sun, Z.-Y.; Zhao, Y.-F.; Kunz, H.; Li, Y.-M. Self-adjuvanting synthetic antitumor vaccines from MUC1 glycopeptides conjugated to T-cell epitopes from tetanus toxoid. *Angew. Chem., Int. Ed.* **2013**, *52*, 6106–6110.
- (24) Wilkinson, B. L.; Day, S.; Chapman, R.; Perrier, S.; Apostolopoulos, V.; Payne, R. J. Synthesis and immunological evaluation of self-assembling and self-adjuvanting tricomponent glycopeptide cancer-vaccine candidates. *Chem. - Eur. J.* **2012**, *18*, 16540–16548.
- (25) Zom, G. G.; Welters, M. J.; Loof, N. M.; Goedemans, R.; Lougheed, S.; Valentijn, R. R.; Zandvliet, M. L.; Meeuwenoord, N. J.; Melief, C. J.; de Gruijl, T. D.; Van der Marel, G. A.; Filippov, D. V.; Ossendorp, F.; Van der Burg, S. H. TLR2 ligand-synthetic long peptide conjugates effectively stimulate tumor-draining lymph node T cells of cervical cancer patients. *Oncotarget* **2016**, *7*, 67087–67100.
- (26) Xu, Z.; Moyle, P. M. Bioconjugation approaches to producing subunit vaccines composed of protein or peptide antigens and covalently attached Toll-like receptor ligands. *Bioconjugate Chem.* **2018**, *29*, 572–586.
- (27) Tyne, A. S.; Chan, J. G.; Shanahan, E. R.; Atmosukarto, I.; Chan, H. K.; Britton, W. J.; West, N. P. TLR2-targeted secreted proteins from *Mycobacterium tuberculosis* are protective as powdered pulmonary vaccines. *Vaccine* **2013**, *31*, 4322–4329.
- (28) Andersson, M.; Lutay, N.; Hallgren, O.; Westergren-Thorsson, G.; Svensson, M.; Godaly, G. *Mycobacterium bovis* bacilli Calmette-Guerin regulates leukocyte recruitment by modulating alveolar inflammatory responses. *Innate Immun.* **2012**, *18*, 531–540.
- (29) Hertz, C. J.; Wu, Q.; Porter, E. M.; Zhang, Y. J.; Weismüller, K.-H.; Godowski, P. J.; Ganz, T.; Randell, S. H.; Modlin, R. L. Activation of Toll-like receptor 2 on human tracheobronchial epithelial cells induces the antimicrobial peptide human β defensin-2. *J. Immunol.* **2003**, *171*, 6820–6826.
- (30) Li, Y.; Wang, Y.; Liu, X. The role of airway epithelial cells in response to *Mycobacteria* infection. *Clin. Dev. Immunol.* **2012**, No. 791392.
- (31) Gupta, N.; VEDI, S.; Kunitomo, D. Y.; Agrawal, B.; Kumar, R. Novel lipopeptides of ESAT-6 induce strong protective immunity against *Mycobacterium tuberculosis*: Routes of immunization and TLR agonists critically impact vaccine's efficacy. *Vaccine* **2016**, *34*, 5677–5688.
- (32) Dawson, P. E.; Muir, T. W.; Clark-Lewis, I.; Kent, S. B. Synthesis of proteins by native chemical ligation. *Science* **1994**, *266*, 776–779.
- (33) Thompson, R. E.; Liu, X.; Alonso-García, N.; Pereira, P. J. B.; Jolliffe, K. A.; Payne, R. J. Trifluoroethanethiol: an additive for efficient one-pot peptide ligation–desulfurization chemistry. *J. Am. Chem. Soc.* **2014**, *136*, 8161–8164.
- (34) Hanna, C. C.; Kulkarni, S. S.; Watson, E. E.; Premjee, B.; Payne, R. J. Solid-phase synthesis of peptide selenoesters via a side-chain anchoring strategy. *Chem. Commun.* **2017**, *53*, 5424–5427.
- (35) Wang, P.; Miranda, L. P. Fmoc-protein synthesis: preparation of peptide thioesters using a side-chain anchoring strategy. *Int. J. Pept. Res. Ther.* **2005**, *11*, 117–123.
- (36) Ficht, S.; Payne, R. J.; Guy, R. T.; Wong, C. H. Solid-phase synthesis of peptide and glycopeptide thioesters through side-chain-anchoring strategies. *Chem. Eur. J.* **2008**, *14*, 3620–3629.
- (37) Saunders, B. M.; Britton, W. J. Life and death in the granuloma: immunopathology of tuberculosis. *Immunol. Cell Biol.* **2007**, *85*, 103–111.

- (38) Zygmunt, B. M.; Rharbaoui, F.; Groebe, L.; Guzman, C. A. Intranasal immunization promotes Th17 immune responses. *J. Immunol.* **2009**, *183*, 6933–6938.
- (39) Orr, M. T.; Beebe, E. A.; E. Hudson, T.; Argilla, D.; Huang, P.-W. D.; Reese, V. A.; Fox, C. B.; Reed, S. G.; Coler, R. N. Mucosal delivery switches the response to an adjuvanted tuberculosis vaccine from systemic Th1 to tissue-resident Th17 responses without impacting the protective efficacy. *Vaccine* **2015**, *33*, 6570–6578.
- (40) Ouyang, W.; Kolls, J. K.; Zheng, Y. The biological functions of T helper 17 cell effector cytokines in inflammation. *Immunity* **2008**, *28*, 454–467.
- (41) Okamoto Yoshida, Y.; Umemura, M.; Yahagi, A.; O'Brien, R. L.; Ikuta, K.; Kishihara, K.; Hara, H.; Nakae, S.; Iwakura, Y.; Matsuzaki, G. Essential role of IL-17A in the formation of a Mycobacterial infection-induced granuloma in the lung. *J. Immunol.* **2010**, *184*, 4414–4422.
- (42) Khader, S. A.; Bell, G. K.; Pearl, J. E.; Fountain, J. J.; Rangel-Moreno, J.; Cilley, G. E.; Shen, F.; Eaton, S. M.; Gaffen, S. L.; Swain, S. L.; Locksley, R. M.; Haynes, L.; Randall, T. D.; Cooper, A. M. IL-23 and IL-17 in the establishment of protective pulmonary CD4⁺ T cell responses after vaccination and during *Mycobacterium tuberculosis* challenge. *Nat. Immunol.* **2007**, *8*, 369–377.
- (43) Noack, M.; Miossec, P. Th17 and regulatory T cell balance in autoimmune and inflammatory diseases. *Autoimmun. Rev.* **2014**, *13*, 668–677.
- (44) Cooper, A. M. Editorial: Be careful what you ask for: is the presence of IL-17 indicative of immunity? *J. Leukocyte Biol.* **2010**, *88*, 221–223.
- (45) Uranga, S.; Marinova, D.; Martin, C.; Aguilo, N. Protective efficacy and pulmonary immune response following subcutaneous and intranasal BCG administration in mice. *J. Vis. Exp.* **2016**, *115*, No. e54440.
- (46) Lindenstrøm, T.; Woodworth, J.; Dietrich, J.; Aagaard, C.; Andersen, P.; Agger, E. M. Vaccine-induced Th17 cells are maintained long-term postvaccination as a distinct and phenotypically stable memory subset. *Infect. Immun.* **2012**, *80*, 3533–3544.
- (47) Wozniak, T. M.; Saunders, B. M.; Ryan, A. A.; Britton, W. J. *Mycobacterium bovis* BCG-specific Th17 cells confer partial protection against *Mycobacterium tuberculosis* infection in the absence of gamma interferon. *Infect. Immun.* **2010**, *78*, 4187–4194.
- (48) McShane, H.; Williams, A. A review of preclinical animal models utilised for TB vaccine evaluation in the context of recent human efficacy data. *Tuberculosis* **2014**, *94*, 105–110.
- (49) Lang, S. B.; O'Nele, K. M.; Douglas, J. T.; Tunge, J. A. Dual catalytic decarboxylative allylations of alpha-amino acids and their divergent mechanisms. *Chem. - Eur. J.* **2015**, *21*, 18589–18593.
- (50) Latz, E.; Visintin, A.; Lien, E.; Fitzgerald, K. A.; Monks, B. G.; Kurt-Jones, E. A.; Golenbock, D. T.; Espevik, T. Lipopolysaccharide rapidly traffics to and from the golgi apparatus with the Toll-like receptor 4-MD-2-CD14 complex in a process that is distinct from the initiation of signal transduction. *J. Biol. Chem.* **2002**, *277*, 47834–47843.